ELSEVIER

Journal of Photochemistry and Photobiology A: Chemistry 117 (1998) 199–207

Journal of Photochemistry and Photobiology A:Chemistry

Nucleotides enhance the fluorescence of *trans*-4-(*p*-*N*,*N*-dimethylaminostyryl)-*N*-vinylbenzylpyridinium chloride

Petra Turkewitsch[a,b], Barbara Wandelt[c,1], Graham D. Darling[c,2], William S. Powell[a,b,*]

[a] *Meakins-Christie Laboratories, Department of Medicine, 3626 St. Urbain Street, Montreal, Quebec, Canada H2X 2P2*

[b] *Montreal Chest Institute Research Center, Department of Medicine, McGill University, 3626 St. Urbain Street, Montreal, Quebec, Canada H2X 2P2*

[c] *Department of Chemistry, McGill University, 801 Sherbrooke St. W., Montreal, Quebec, Canada H3A 2K6*

Received 2 April 1998; received in revised form 11 June 1998; accepted 12 June 1998

Abstract

The newly synthesized *trans*-4-(*p*-*N*,*N*-dimethylaminostyryl)-*N*-vinylbenzylpyridinium chloride (**1**) displays strong solvatochromic behavior resulting from a large increase of ~18 D in its dipole moment upon excitation. This indicates that its excited state has considerable charge transfer character, suggesting that it may be subject to solute-induced fluorescence changes. The fluorescence quantum yield of **1** is enhanced dramatically (12-fold) in the presence of a buffered aqueous solution of cAMP, a purine nucleotide. In contrast, the pyrimidine nucleotides, CMP and UMP, have virtually no effect on the fluorescence of **1**. cGMP induced an increase in the quantum yield of **1** similar to that induced by cAMP, whereas other purine nucleotides (AMP, ADP and ATP) and adenosine induced changes of somewhat lesser magnitude. Association constants for **1** with these analytes ranged from 13.8 M^{-1} for cAMP to 0.15 M^{-1} for adenine. We conclude that the changes in fluorescence of **1** in the presence of nucleotides require the presence of a purine base, and are enhanced by ribose and phosphate moieties. The environmentally sensitive fluorescence of **1** suggests that such compounds may be useful as chemosensors for purine nucleotides.

Keywords: Dimethylaminostyrylpyridinium dye; Solvatochromism; Fluorescence enhancement; Nucleotides; Chemosensor; Charge transfer

1. Introduction

Fluorescent indicators are perhaps the most popular and powerful tools for the measurement of intracellular concentrations of various ions and other messengers involved in the transduction of biological signals [1]. The virtue of fluorescence is that it can be applied to intact cells with high spatial and temporal resolution while the cells undergo physiological responses [1]. To this end, sensor molecules that communicate their association with analytes fluorometrically are attracting considerable attention [1]. In particular, electron donor–acceptor (EDA) molecules have been employed as chemosensors for ions, [2] micelles, [3–5] polymeric matrices [4,6] and biological systems, [7–9] since they display fluorescence from intramolecular charge transfer (ICT) excited states, which are known to be remarkably sensitive to the microenvironment [10,11].

The environmental sensitivity of fluorescent EDA stilbene [3,12] and styrylpyridinium [4,9,13–15] molecules, prompted us to synthesize **1**, which combines the special photophysical properties of these EDA molecules with a positive charge capable of promoting an association with negatively charged nucleotides. We are particularly interested in the cyclic nucleotide, adenosine 3′:5′-cyclic monophosphate (cAMP), because of its vital role as an intracellular second messenger, mediating the actions of many hormones, drugs and neurotransmitters which act via cell surface receptors [16]. The presence of the vinyl group permits the use of dye **1** for the preparation of fluorescent molecularly imprinted polymer chemosensors [17].

Recently, we reported [18] a marked fluorescence quantum yield enhancement of **1** in the presence of unbuffered aqueous solutions of cAMP and cGMP, suggesting that dye **1** preferentially associates with these cyclic nucleotides. The objectives of the present study were to further explore the environmentally sensitive fluorescence of **1** under more relevant biological conditions, which would allow investigation into the nature of the association between dye **1** and nucleotides in the physiological pH range, and examination

*Corresponding author. Tel.: +1-514-398-3864; fax: +1-514-398-7483; e-mail: bill@meakins.lan.mcgill.ca

[1]Present address: The Technical University, Institute of Polymers, Lodz, Poland 90924.

[2]Present address: Active Materials Inc., P.O. Box 47, Russell (Ottawa), ON, Canada K4R 1C7.

1010-6030/98/$ – see front matter
PII: S1010-6030(98)00338-4

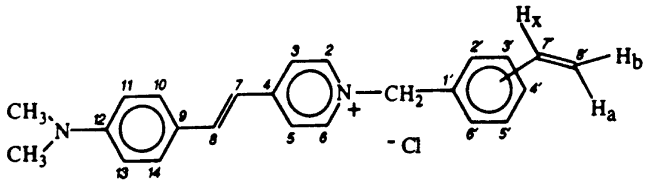

1

Fig. 1. Molecular structure of *trans*-4-(*p*-*N*,*N*-dimethylaminostyryl)-*N*-vinylbenzylpyridinium chloride (**1**) (70:30 mixture of *m*-vinylbenzyl:*p*-vinylbenzyl isomers).

of the structural requirements for the effects of the nucleotides on the quantum yield of **1**. We found that dye **1** shows dramatic fluorescence enhancements in the presence of purine nucleotides, but almost no fluorescence enhancement with pyrimidine nucleotides. Thus, dye **1** could be a prototype for fluorescent chemosensors for purine nucleotides such as cAMP.

2. Experimental

2.1. Materials

4-(*p*-Dimethylaminostyryl)pyridine (DMASP) was prepared by a published procedure [19]. 3-Vinylbenzyl chloride (70:30 mixture of *m*-vinylbenzyl chloride:*p*-vinylbenzyl chloride) was purchased from the Aldrich Chemical and used without further purification. The nucleotides: adenosine 3′:5′-cyclic monophosphate sodium salt (cAMP), guanosine 3′:5′-cyclic monophosphate sodium salt (cGMP), adenosine 5′-monophosphate sodium salt (AMP), adenosine 5′-diphosphate sodium salt (ADP), adenosine 5′-triphosphate disodium salt (ATP), cytidine 5′-monophosphate disodium salt (CMP), and uridine 5′-monophosphate (UMP), as well as adenosine were used as received from the Sigma. D-ribose-5-phosphate disodium salt dihydrate 95%, and adenine hydrochloride hemihydrate (99%, 'adenine') were used as received from the Aldrich Chemical. Aqueous solutions were prepared using double distilled deionized water (Millipore). Buffer solutions were prepared from monobasic sodium phosphate, anhydrous dibasic sodium phosphate, and fused-anhydrous sodium acetate, all purchased from Fisher Scientific. Organic solvents used in synthesis were reagent grade or better. Solvents employed in spectroscopic measurements were 'Spectrograde'.

2.2. Methods

The ^{1}H NMR and ^{13}C NMR spectra were recorded on Varian Unity-500 and Varian XL-300 spectrometers, respectively. Elemental analysis was performed by Robertson Microlit Laboratories, Madison, NJ. UV-VIS absorption spectra were recorded on a Beckmann DU-64 spectrophotometer. Fluorescence spectra were measured on a photon technology international (PTI) Deltascan 4000 spectrofluorometer with 8 nm emission slits on solutions in 1 cm rectangular cuvettes maintained at 22±0.1°C. Excitation wavelengths of 469 and 360 nm were used to obtain the fluorescence emission spectra of **1** in solutions. The fluorescence quantum yield of dye **1** in all solutions was determined by the method of Parker and Rees [20] from the emission spectrum obtained with excitation at 469 or 360 nm relative to the quantum yield of rhodamine B in ethanol (Φ=0.69; excitation=366 nm; 22°C) as a standard. The integrated areas under the emission bands gave the relative intensities of the solutions. The quantum yields were calculated with corrections for the absorbances of all solutions [20]. A low concentration of dye (10^{-5} M), which gave absorbances of less than 0.3 absorbance units at the exciting wavelength, was used to minimize the contributions of self-absorption and self-aggregation. To quantify the components in the fluorescence spectra of **1** obtained at 360 nm excitation, curve-fitting was performed, assuming a Gaussian distribution and using a non-linear least squares method based on the Marquardt–Levenberg algorithm, with goodness of fit checked using standard deviation, residuals intensity and the coefficient of determination r^2, by means of Jandel Scientific's PEAKFIT software.

2.3. Preparation of solutions

The concentration of dye **1** in solvents used for the determination of the change in its dipole moment between the ground and excited states was 10^{-5} M, except in tetrahydrofuran where the concentration was lower due to solubility limitations. Solutions containing various concentrations of cAMP, cGMP, AMP, ADP, ATP, CMP, UMP, adenosine, adenine, and D-ribose-5-phosphate, with a constant concentration (10^{-5} M) of dye **1** were prepared in 0.5 M phosphate or acetate buffer. Spectroscopic measurements were performed the following day on thoroughly mixed nondegassed solutions.

2.4. *Trans*-4-(*p*-*N*,*N*-dimethylaminostyryl)-*N*-vinylbenzylpyridinium chloride (**1**)

Acetonitrile (10 ml) was added to a round bottom flask equipped with a magnetic stirrer, reflux condenser topped with a nitrogen inlet, and heating mantle, and containing DMASP (0.246 g, 1.10 mmol). While flushing with nitrogen and stirring, the temperature was slowly raised to 60°C. 3-Vinylbenzyl chloride (0.251 g, 1.68 mmol) was then added dropwise over ~15 min to give an orange reaction mixture. After gentle refluxing for ~48 h under nitrogen, any remaining undissolved starting material was filtered off, leaving a clear deep red mother liquor which was rotoevaporated to dryness. The product Fig. 1 was recrystallized from methylene chloride and carbon tetrachloride and dried under vacuum (20 mm Hg) at 35°C overnight, yielding 0.280 g (68%) of dark red crystals which were stored in a desiccator

in the dark. Melting point=225–227°C; one spot by TLC (ethanol:toluene 3:7/SiO_2); ^{1}H NMR (500 MHz, $CDCl_3$) δ 3.04 ppm (s, 6H, *CH₃*), 5.24 ppm (d, 1H, $H_b^{8'}$, J=11 Hz), 5.69 ppm (d, 0.3H, *para* $H_a^{8'}$, J=17.3 Hz), 5.78 ppm (d, 0.7H, *meta* $H_a^{8'}$, J=17.6 Hz), 6.01 ppm (s, 2H, CH_2), 6.62 ppm (m, 1H, $H^{7'}$), 6.67 ppm (d, 2H, $H^{11,13}$), 6.77 ppm (d, 1H, H^7, J=15.8 Hz), 7.28 ppm (t, 0.7H, *meta* $H^{5'}$, J=7.2 Hz), 7.34 ppm (d, 1.3H, *meta* $H^{4'}$ and *para* $H^{3',5'}$), 7.47 ppm (d, 2H, $H^{10,14}$), 7.49 ppm (d, 0.7H, *meta* $H^{6'}$), 7.52 ppm (d, 1H, H^8), 7.58 ppm (d, 0.6H, *para* $H^{2',6'}$, J=7.3 Hz), 7.63 ppm (s, 0.7H, *meta* $H^{2'}$), 7.73 ppm (d, 2H, $H^{3,5}$), 9.19 ppm (d, 2H, $H^{2,6}$); ^{13}C NMR (75.43 MHz, $CDCl_3$) 40.2 (CH_3), 62.5 (CH_2), 112.2 ($C^{11,13}$), 115.3 (*para* $C^{8'}$), 115.5 (*meta* $C^{8'}$), 116.6 (C^7), 122.6 ($C^{3,5}$), 127.1 (*meta* $C^{2',4'}$ and *para* $C_{3',5'}$), 128.6 (*meta* $C^{6'}$), 129.6 (*meta* $C^{5'}$ and *para* $C_{2',6'}$), 130.6 ($C^{10,14}$), 135.7 ($C^{7'}$), 133.1, 134.1, 135.8, 138.7 (*meta* $C^{1',3'}$, *para* $C^{1',4'}$ and C^9), 142.8 (C^8), 143.6 ($C^{2,6}$), 152 (C^{12}), 154 (C^4); Anal. Calc. for $C_{24}H_{25}N_2Cl{\cdot}0.75\ H_2O$: C, 73.83; H, 6.84; N, 7.18. Found C, 73.62; H, 6.57; N, 6.86.

3. Results

3.1. Absorption and fluorescence spectra of 1

Fig. 2 shows the UV-Vis absorption spectra of **1** in phosphate buffer (pH 7.2). The single broad absorption band of **1** exhibited a λ_{max} at 469 nm with a molar extinction coefficient of 21 300 l mol^{-1} cm^{-1}, very similar to that obtained in water [18]. The fluorescence spectra of **1** in phosphate buffer (pH 7.2) at excitation 469 and 360 nm are presented in Fig. 3. Irradiation of **1** at 469 nm generated a single structureless emission band with a maximum at 608 nm, and a quantum yield of 1.18×10^{-3} (Fig. 3(a)). This band is very similar to that obtained in unbuffered water at excitation 469 nm [18]. Excitation of **1** at 360 nm resulted in a broad structured emission spectrum (Fig. 3(b)) that could be decomposed by curve-fitting analysis (r^2>0.995, standard error±10%) into two Gaussian emission peaks with local maxima at 502 and 602 nm, and quantum yields of 3.66×10^{-4} and 6.93×10^{-4}, respectively. The intensity of this dual emission was about an order of magnitude lower than that obtained by exciting at 469 nm. A similar emission spectrum was obtained in unbuffered water by exciting at 360 nm (unpublished results). The deconvoluted peak with a maximum at 602 nm appeared to be similar to the single emission band obtained at excitation 469 nm.

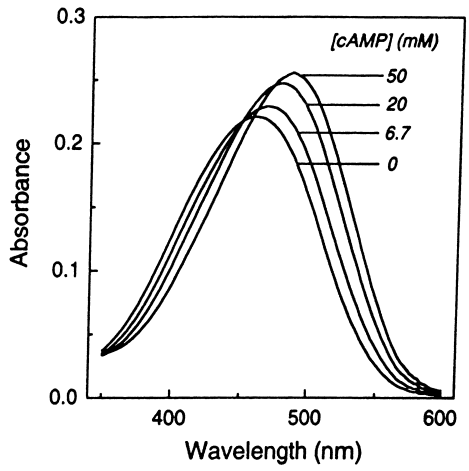

Fig. 2. Absorption spectra of **1** (10^{-5} M) in 0.5 M phosphate buffer (pH 7.2) in the absence and presence of various concentrations of cAMP (6.67, 20 and 50 mM).

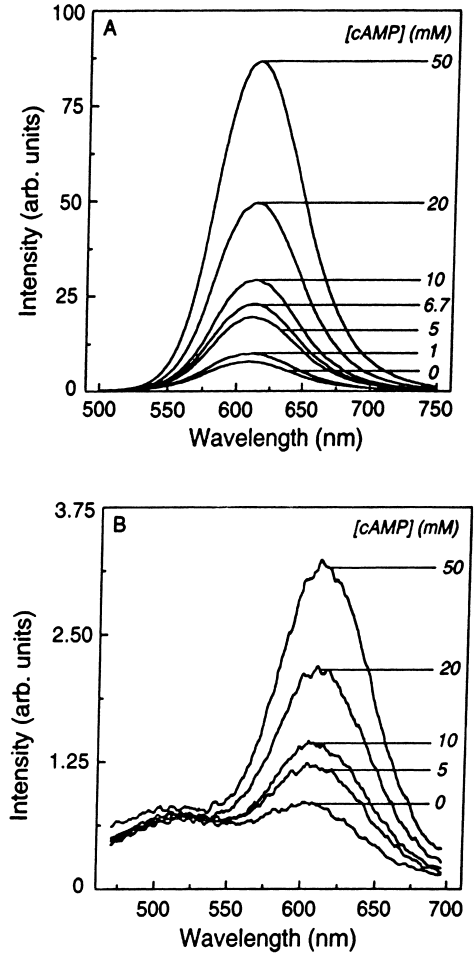

Fig. 3. Fluorescence spectra of **1** (10^{-5} M) in 0.5 M phosphate buffer (pH 7.2) at excitation wavelengths of 469 nm (a) and 360 nm (b) in the absence and presence of various concentrations of cAMP (1, 5, 6.67, 10, 20, 50 mM). At excitation 469 nm the emission maxima varied between 608 and 613 nm; at excitation 360 nm the emission maximum at 502 nm remained constant, whereas that at 602 nm varied between 602 and 613 nm.

3.2. Determination of the change in the dipole moment between the ground and excited states ($\Delta\mu_{eg}$) of 1

The main characteristics of the UV-VIS and fluorescence spectra of **1** in various solvents together with some solvent

Table 1
Solvent parameters and steady-state spectral data for **1**[a] in aprotic (1–6) and protic (7–10) solvents

Number	Solvent	ε[b]	η[c]	Δf[d]	λ_a^e (nm)	λ_f^f (nm)	ν_{st}^g (cm^{-1})
Aprotic							
1	Chloroform	4.81	1.4429	0.1492	500	571	2487
2	Tetrahydrofuran	7.58	1.4072	0.2096	480	582	3651
3	*N*,*N*-dimethylformamide	12.47	1.3877	0.2514	482	618	4566
4	Dimethyl sulfoxide	46.68	1.4783	0.2634	484	621	4558
5	Acetone	20.70	1.3587	0.2843	484	613	4348
6	Acetonitrile	37.50	1.3441	0.3054	482	613	4434
Protic							
7	2-propanol	19.92	1.3772	0.2762	495	600	3535
8	Ethanol	24.55	1.3614	0.2887	491	606	3865
9	Methanol	32.70	1.3284	0.3086	488	606	3990
10	Water	78.39	1.3330	0.3199	469	610	4929

[a] Concentration 10^{-5} M, except in tetrahydrofuran where solubility was lower.
[b] Dielectric constant, ε, obtained from [21].
[c] Refractive index, η, obtained from [21].
[d] Solvent polarity function, $\Delta f = (\varepsilon - 1/(2\varepsilon + 1)) - (\eta^2 - 1/(2\eta^2 + 1))$, defined in Eq. (1).
[e] Absorption maximum, λ_a; maximum uncertainty ±2 nm.
[f] Fluorescence maximum, λ_f; maximum uncertainty ±2 nm; excitation wavelength 469 nm.
[g] Stokes' shift calculated from difference in absorption and fluorescence maxima; maximum uncertainty ±300 cm^{-1}.

polarity parameters are reported in Table 1. Dye **1** exhibits a large Stokes' shift (ν_{st}) which is solvent dependent, suggesting that the excited state reached upon excitation at 469 nm has substantial CT character, analogous to related derivatives [12,15,22].

Within the dielectric continuum approximation of the solvent, the steady-state Stokes' shift, ν_{st} (in cm^{-1}), may be related to the change in the dipole moment between the ground and the excited states, $\Delta\mu_{eg}$, of **1** according to the Lippert–Mataga Eq. (1)[23].

$$\nu_{st}\,(cm^{-1}) = \nu_a - \nu_f = 2\frac{(\Delta\mu_{eg})^2}{hca^3}\left[\frac{\varepsilon - 1}{2\varepsilon + 1} - \frac{\eta^2 - 1}{2\eta^2 + 1}\right] + A = 2\frac{(\Delta\mu_{eg})^2}{hca^3} \times \Delta f + A \quad (1)$$

In the above equation, ν_a and ν_f, refer to the maximum frequencies of the absorption and emission spectra, respectively; h is Planck's constant; c is the speed of light; a is the spherical solvent cavity radius of the solute; ϵ and η are the dielectric constant and refractive index of the solvent, respectively; and A is a constant. The Lippert–Mataga analysis of the steady-state spectroscopic data for **1** is shown in Fig. 4. The steady-state Stokes' shift for **1** is best approximated by a linear function if the solvents are divided into two groups, protic and aprotic. These results suggest that specific solvent–solute interactions may occur in protic solvents and influence the steady-state Stokes' shift [15,24]. The magnitude of $\Delta\mu_{eg}$ may be obtained from the slopes of the ν_{st} vs. Δf plots in Fig. 4 by estimating the value of the solute radius, a (5.40 Å), from the molecular volume as calculated from the molecular weight and the density of *N*,*N*-dimethylaniline (0.95 g cm^{-3}) [12]. Least-squares fits to the plots give the following slopes for protic and aprotic solvents, respectively: 2.73×10^4 $cm^{-1}/\Delta f$ (r=0.90) and 1.32×10^4 $cm^{-1}/\Delta f$ (r=0.91). These slopes yield dipole moment changes of 20.69 and 14.39 Debye units (D) (1 D=3.33×10^{-30} C m) for protic and aprotic solvents, respectively. Considering the large $\Delta\mu_{eg}$, it is reasonable to conclude that the excited state of **1** has considerable CT character.

3.3. Effect of nucleotide and nucleotide-related analytes on the absorption and fluorescence of **1**

Fig. 2 also shows the UV-Vis absorption spectra of **1** in phosphate buffer (pH 7.2) in the presence of various

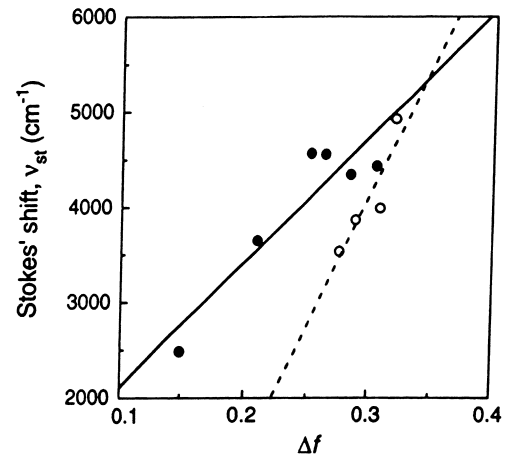

Fig. 4. Lippert–Mataga plots of the Stokes' shift (in cm^{-1}), ν_{st}, vs. the solvent polarity function, Δf, for **1**: aprotic solvents (●, 1–6 in Table 1) slope=1.32×10^4 $cm^{-1}/\Delta f$, r=0.91; protic solvents (○, 7–10 in Table 1) slope=2.73×10^4 $cm^{-1}/\Delta f$, r=0.90. The lines are linear least-squares fits through the aprotic and protic solvents.

concentrations of cAMP. The addition of increasing concentrations of cAMP caused a red shift of ~17 nm in the absorption maximum accompanied by a hyperchromic effect, which could be observed visually as a change from orange to red–orange. All other nucleotide and nucleotide-related analytes induced similar changes in the absorbance of **1**, whereas D-ribose-5-phosphate had no effect (data not shown). Concentrations of analyte above 50 mM were not examined due to solubility limitations. These changes were also observed for **1** in unbuffered water upon addition of cAMP, cGMP and D-ribose-5-phosphate [18].

The addition of cAMP induced a dramatic concentration-dependent enhancement in the fluorescence quantum yield of **1** at excitation 469 nm with a concomitant slight red shift of the λ_{max} from 608 nm in buffer alone to 613 nm at 50 mM cAMP (Fig. 3(a)). The quantum yield of the emission band of **1** with maximum at 602 nm obtained by exciting at 360 nm also increased as the concentration of cAMP increased (Fig. 3(b)). This increase in fluorescence was accompanied by a slight red shift of the λ_{max} from 602 in buffer alone to 613 nm in the presence of 50 mM cAMP, reminiscent of the emission band produced upon excitation at 469 nm. However, it was less sensitive to the presence of cAMP than the similar peak arising from the 469 nm excitation. In contrast, the emission band of **1** with a maximum at 502 nm obtained by exciting at 360 nm remained relatively constant as the concentration of cAMP was increased.

Fig. 5 shows the fluorescence quantum yield titration curves obtained at excitation 469 nm when various concentrations of nucleotide and nucleotide-related analytes were added to **1** (10^{-5} M) in phosphate buffer (pH 7.2). These

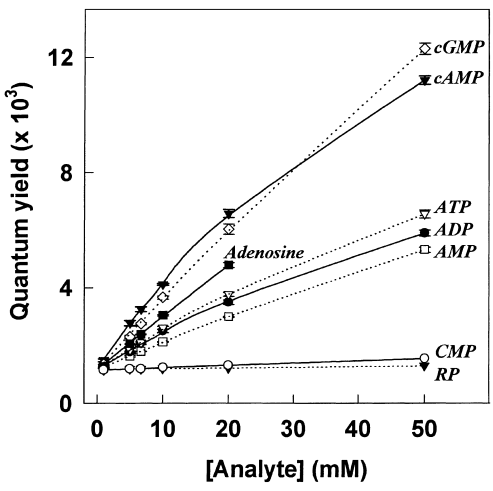

Fig. 5. Fluorescence quantum yield titration curves of **1** as a function of analyte concentration. Phosphate buffer solutions (0.5 M, pH 7.2) contained **1** (10^{-5} M) and various concentrations of cGMP (◇), cAMP (▼), adenosine (■), ATP (▽), ADP (●), AMP (□), CMP (▲) or D-ribose-5-phosphate (RP, ○). The lines through the symbols for cAMP, cGMP, AMP, ADP and ATP represent curve fits following Eq. (3). The excitation wavelength was 469 nm. The values are means ±standard errors of three independent observations.

concentration-response curves show that the purine nucleotides (cAMP, cGMP, AMP, ADP, and ATP) and adenosine all induce a fluorescence quantum yield enhancement of **1**. In contrast, the pyrimidine nucleotide, CMP, has virtually no effect on quantum yield. UMP, another pyrimidine nucleotide, behaved almost identically to CMP (data not shown). D-ribose-5-phosphate has no effect on the fluorescence of **1**. Of the purine nucleotides, the cyclic nucleotides, cAMP and cGMP have the greatest effects on the fluorescence quantum yield of **1** whereas the noncyclic nucleotides, AMP, ADP and ATP have somewhat smaller effects. Adenosine has an effect intermediate between those of the cyclic and noncyclic nucleotides. However, it was not possible to examine concentrations of adenosine above 20 mM due to solubility limitations.

The data in Fig. 5 can be used to calculate the equilibrium association constant (K_{eq}) for the interaction of dye **1** with analyte, as well as the fluorescence quantum yield (Φ_c) of the dye–analyte complex. The association of dye with analyte, dye + analyte $\rightleftharpoons$ dye − analyte, is controlled by the equilibrium association constant:

$$K_{eq} = \frac{[\text{dye} - \text{analyte}]}{[\text{dye}][\text{analyte}]} \quad (2)$$

In the concentration range studied, the fluorescence quantum yield is closely correlated with the concentrations of the analytes. The data were analyzed following the equation

$$\Phi = \Phi_0 + (\Phi_c - \Phi_0)\left(\frac{K_{eq}[\text{analyte}]}{1 + K_{eq}[\text{analyte}]}\right) \quad (3)$$

The fluorescence quantum yield Φ of **1** in the presence of analyte represents the quantum yield of a mixture of fluorescing species, which may be described by the equation

$$\Phi = x_{dye}\Phi_0 + (1 - x_{dye})\Phi_c \quad (4)$$

where x_{dye} is the mole fraction of 'free' dye **1**, and Φ_0 and Φ_c are the fluorescence quantum yields of **1** in the absence of analyte, and of the dye–analyte complex, respectively. Eq. (3) was easily derived from Eqs. (2) and (4) and the definitions of the mole fractions of the fluorescing species. SIGMAPLOT curve fitter was used to fit the fluorescence titration data in Fig. 5 to Eq. (3) directly to determine the K_{eq} and Φ_c values. Table 2 presents these values obtained in phosphate buffer at 7.2 and in unbuffered water [18].[3]

The association constants obtained in phosphate buffer at pH 7.2 (Table 2) range from 13.8 for cAMP to 0.15 M^{-1} for adenine. To compare the effects of the adenine base alone to those of the nucleotides, the pH had to be lowered to 4.0 to dissolve the adenine. Under these conditions, cAMP exhibited a K_{eq} value (13.0 M^{-1}) similar to the those in phosphate buffer and unbuffered water, whereas adenine exhibited an association constant of 0.15 M^{-1}, much less than that of

[3]The equilibrium association constants for cAMP and cGMP in water were calculated incorrectly in [18]. The corrected values are presented in Table 2.

Table 2
Equilibrium association constants (K_{eq})[a] for **1** with various analytes and the fluorescence quantum yields of the dye–analyte complexes (Φ_c) in 0.5 M phosphate buffer at pH 7.2 and in unbuffered water[b]

Analyte	Phosphate buffer[c]		Water[c]	
	K_{eq}	Φ_c	K_{eq}	Φ_c
cAMP	13.8±0.80	0.026±0.001	14.0±1.08	0.018±0.0003
cGMP	2.67±0.35	0.099±0.009	9.31±0.97	0.031±0.004
AMP	3.81±1.12	0.031±0.007	–	–
ADP	10.1±0.79	0.015±0.001	–	–
ATP	8.08±0.73	0.020±0.001	–	–
Adenosine	0.54±0.10	0.373±0.067	–	–
Adenine[d]	0.15±0.01	0.331±0.005	–	–

[a] Units (M^{-1}).
[b] [18], see [3] in text.
[c] Values are means±standard error of three independent observations.
[d] In 0.5 M acetate buffer at pH 4.0. The K_{eq} and Φ_c for cAMP under these conditions were 13.0 M^{-1} and 0.023, respectively.

cAMP. The equilibrium constant for cAMP in unbuffered water [18] resembles that in phosphate buffer, whereas the K_{eq} for cGMP in water is somewhat greater than that in phosphate buffer.

In contrast to the relatively low apparent affinities of adenine and adenosine for **1**, the quantum yield for their dye–analyte complex (Φ_c∼0.35) was higher than that for any of the purine nucleotides tested. However, this result must be interpreted with caution since we could not use concentrations of adenine or adenosine in excess of 20 mM due to their limited solubilities. Similarly, cGMP, although it has a lower K_{eq} than cAMP, induces a greater change in the quantum yield of **1** at the highest concentration tested; the value of Φ_c for cGMP is nearly 4 times that for cAMP. The values of Φ_c for AMP, ADP and ATP were similar to that for cAMP at pH 7.2 (Table 2) as well as at pH values of 6.0 and 8.0 (Table 3). Similarly, the K_{eq} values for these nucleotides were not influenced to a large extent by pH (Table 3).

4. Discussion

The similarity of the molecular structure of **1** with those of closely related EDA stilbene [12,22] and styrylpyridinium [4,14,15] dyes, suggests that **1** may form a twisted intramolecular charge transfer (TICT) excited state. As with most molecules exhibiting TICT behavior, dye **1** contains several possible rotatable moieties with excellent donor properties, linked to acceptor groups. TICT excited states may form in flexible EDA molecules where the possibility of rotation of the donor and acceptor groups around certain bonds exists [10]. In some of these cases, upon excitation at a single wavelength dual fluorescence may be observed from two configurations of the same molecule: an initially planar locally excited (LE) state, and a TICT excited state in which a charge transfer from the donor group to the acceptor group has taken place with a twisting of the donor towards a plane perpendicular to that of the acceptor. The high degree of charge separation between the donor and acceptor moieties in the excited molecule leads to an abrupt increase in the dipole moment with respect to the ground state [10].

Recent studies on a fluorescent EDA molecule, *trans*-4-(*p*-*N*,*N*-dimethylamino)stilbene (DAS),[12] similar to dye **1**, revealed the occurrence of a TICT excited state. Moreover, we [13] reported that *trans*-4-(*p*-*N*,*N*-dimethylaminostyryl)-*N*-phenethylpyridinium bromide, which differs from dye **1** only in the substituent on the pyridinium nitrogen, displayed two charge transfer fluorescence bands (close to 600 nm) associated with different excitations, 360 and 469 nm. Our studies suggested that the emission band obtained by exciting at 360 nm, which is part of a broad structured emission spectrum, may arise by a TICT process. The single emission band observed upon excitation at 469 nm may arise from direct excitation of an already twisted ground state, providing an alternative route to a TICT-type emission similar to that obtained by 360 nm excitation.

A difficulty which may be encountered in identifying the TICT process in flexible donor–acceptor compounds is that two distinct emission bands (dual fluorescence) are not always observed in steady-state fluorescence experiments [10]. Here, however, the readily visible dual emission of dye **1** with maxima at 502 and 602 nm observed upon exciting at 360 nm (Fig. 3(b)) further suggests a TICT process in this compound. In addition, the sensitivity of the emission band with a maximum at 602 nm to cAMP (albeit much less than that obtained upon exciting at 469 nm) also implies its origin from a TICT excited state. On the other hand, the insensitivity of the 502 nm emission band to the environment, especially to an environment which possesses highly polar species, suggests that it may be due to a planar locally excited state. Furthermore, the environmental sensitivity of the emission band of **1** with a maximum at ∼600 nm obtained by exciting at 469 nm would also support the idea that it originates from some kind of ICT state.

The average change in the dipole moment (ie. $\Delta\mu_{eg}$) of **1** in both protic and aprotic solvents was calculated to be ∼18 D from solvatochromic measurements. This large value of $\Delta\mu_{eg}$ for **1** further supports the assignment of a TICT nature to this compound. These results are consistent with those of others who have reported similar large $\Delta\mu_{eg}$ values

Table 3
Equilibrium association constants (K_{eq})[a] for **1** with various analytes and the fluorescence quantum yields of the dye–analyte complexes (Φ_c) in 0.5 M phosphate buffer at pH 6.0 and 8.0[b]

Analyte	pH 6.0		pH 8.0	
	K_{eq}	Φ_c	K_{eq}	Φ_c
cAMP	14.1	0.022	16.7	0.020
cGMP	2.57	0.092	1.62	0.130
AMP	6.67	0.028	4.87	0.019
ADP	6.64	0.021	8.56	0.016
ATP	7.27	0.021	11.8	0.014

[a] Units (M^{-1}).
[b] Values are the result of a single observation.

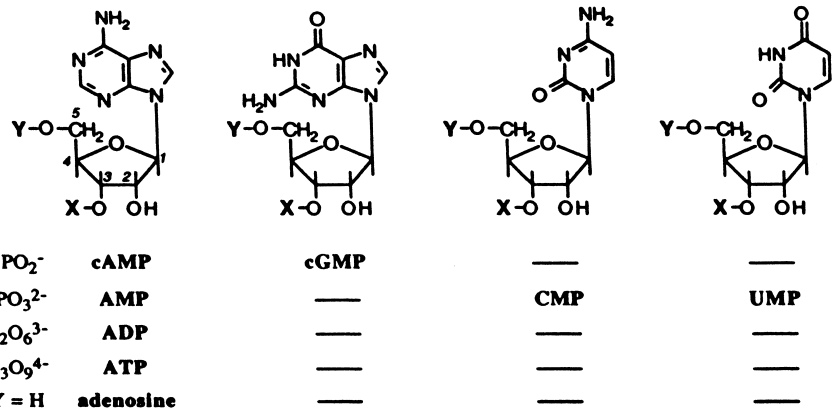

Fig. 6. Molecular structures of the various purine and pyrimidine nucleotides.

for molecules which exhibit TICT excited states, including DAS (10 D), [12] 4-(*N*,*N*-dimethylamino)-4′-cyanostilbene (15 D), [22] and a donor–acceptor-type stilbene laser dye (20 D) [25]. Based on the studies of DAS, the large change in the dipole moment of **1** is probably due to a charge transfer from the dimethylanilino donor group to the vinylpyridinium acceptor moiety in the excited state [12].

The large change in the dipole moment of **1** upon excitation, along with the considerations discussed above would all be consistent with a TICT-type excited state being responsible for the emission of **1** at ~600 nm. This environmentally sensitive fluorescence suggests that **1** may be useful as a chemosensor.

The structures of the analytes investigated are presented in Fig. 6. The nucleotides (cAMP, cGMP, AMP, ADP, ATP, CMP and UMP) consist of a purine or pyrimidine base, a ribose sugar and a phosphate group. However, the nature of the phosphate group differs among them: cAMP and cGMP possess cyclized phosphate groups whereas the other nucleotides have uncyclized phosphates. Adenosine consists of an adenine base linked to a ribose sugar, and D-ribose-5-phosphate consists of a ribose sugar and a phosphate group.

The data in Fig. 5 indicate that dye **1** displays a specificity for purine over pyrimidine analytes in the concentration range studied (1–50 mM), since all of the purine analytes induce a fluorescence quantum yield enhancement of **1**, whereas the pyrimidine analytes have almost no effect. We [13] have previously shown that high solution viscosities can enhance the fluorescence of dyes structurally related to **1**. However, this could not explain the effects of purine nucleotides, since equivalent concentrations of pyrimidine nucleotides did not effect the fluorescence of **1** significantly. It is clear that neither the ribose nor the phosphate groups alone are responsible for the change in fluorescence quantum yield of **1**, since the quantum yield of **1** is unaffected by D-ribose-5-phosphate and phosphate. The results in Table 2 further indicate that the adenine base alone is not capable of interacting strongly with **1**, since adenine displays a K_{eq} of only 0.15 M^{-1}. The addition of a ribose to give adenosine results in an increase in the K_{eq} to 0.54 M^{-1}; and the further addition of a noncyclic phosphate group (AMP) dramatically increases the K_{eq} to 3.81 M^{-1}. Cyclization of the phosphate group further increases the affinity of the nucleotide for **1**, resulting in a higher K_{eq} value for cAMP (13.8 M^{-1}) than for AMP, ADP and ATP. It is possible that the cyclic phosphate group is in a more favorable conformation to interact with the positively charged dye **1**. Thus, the adenine base, the ribose and the phosphate groups appear to act synergistically to increase the affinity of the ligand for the dye. The association of **1** with the purine analytes probably involves concurrent aryl stacking interactions and electrostatic interactions. Aryl stacking interactions could occur between the aromatic rings of **1** and the purine base of the analytes, whereas electrostatic interactions could occur between charged **1** and the phosphate and/or ribose sugar moieties of the analytes, in a multiple-point binding to **1**.

Although the magnitude of the fluorescence changes induced in dye **1** by cAMP and cGMP were similar within the concentration range investigated, curve fitting of the data in Fig. 5 suggested that the K_{eq} and Φ_c for these two nucleotides were substantially different from one another. The K_{eq} calculated for cAMP (13.8 M^{-1}) was about five times higher than that for cGMP (2.67 M^{-1}), but this was offset by the higher value of Φ_c calculated for cGMP (0.099 vs. 0.026 for cAMP). The concentrations of nucleotides required to induce maximal fluorescence changes in dye **1** would be far in excess of those used in our studies, since it was not feasible to use concentrations of cAMP or cGMP greater than 50 mM. Therefore, the values calculated for K_{eq} and Φ_c for the interactions of these compounds with dye **1** must be interpreted with some caution. However, in support of the calculated values, the reproducibility of the measurements was very high, as seen from the error bars in Fig. 5. It might be argued that the calculated values for K_{eq} and Φ_c are overly influenced by the data from the highest concentration (50 mM) of cAMP and cGMP, which was the only concentration at which the fluorescence of dye **1** was greater in the presence of cGMP than cAMP. However, similar results were obtained even when the data for this concentration

were excluded. This would suggest that although cGMP appears to have a lower affinity than cAMP for dye **1**, it can induce a greater maximal increase in fluorescence. To confirm this, further studies would be required to measure lifetimes.

A water-soluble nonfluorescent chemosensor with multiple recognition sites for cAMP was reported by Kato et al. [26]. Its modular structure combined a water-soluble version of Kemp's triacid imide which chelates the adenine base through simultaneous Watson–Crick and Hoogsteen hydrogen bonding and aryl stacking interactions, with a guanidinium moiety for electrostatic interaction with the phosphate group. Equilibrium constants of association, determined by ^{1}H NMR titration, of 600 and 320 M^{-1} in 10 mM cacodylate buffer, 1.0 mM aerosol O.T. at ionic strengths of 51 and 501 mM NaCl, respectively, were reported for this receptor with 3′:5′-cAMP. Hosseini et al. [27] designed a multifunctional receptor capable of binding and hydrolyzing ATP in aqueous solution. The binding of ATP was due to attractive electrostatic interactions between its polyphosphate chain and the positively charged macrocyclic polyammonium moiety of the receptor together with stacking interactions between the acridine side-chain of the latter and the purine base of the nucleotide. The strong acridine fluorescence of this receptor was enhanced by a factor of ~1.9 upon complexation of ATP and CTP, whereas GTP and AMP caused a slight quenching. Furthermore, Kawai et al. [28] stated that a strong tendency of association through aryl-stacking interactions, reportedly dominated by electrostatics, can be expected from similar long and planar structures such as nitrostyrylpyridinium molecules which possess extensive charge delocalization favoring electronic interactions.

The main path of nonradiative deactivation of stilbene derivatives, including DAS, is known to be via rotation around the ethylenic double bond in the excited state, associated with *trans–cis* photoisomerization [12,29]. Environments that restrict this internal molecular rotation of these molecules in the excited state, such as viscous solvents, [14,15] and microheterogeneous micelle [4] and cyclodextrin structures, [30] lead to a decrease in the nonradiative decay rate and consequently an increase in the fluorescence quantum yield. In addition, increases in fluorescence quantum yield and lifetime have been reported for dimethylaminostilbene [12,22] and (dimethylaminostyryl)pyridinium [4,14,15] molecules by 'chemical' or 'physical freezing' of torsional motion around the ethylenic double bond in the excited state. The presence of environmental components capable of associating with these stilbene sensors, may also rigidify their molecular structure, causing fluorescence enhancement [29]. Such enhanced fluorescence emission was reported for *trans*-3,3′-stilbenediboronic acid upon forming a cyclic complex with disaccharides and subsequent freezing of the rotation around the ethylenic bond [29]. Given this, we propose that dye **1** associates with purine analytes in such a way that the rotation about the double bond in the excited state is restricted, inhibiting nonradiative decay and increasing the fluorescence quantum yield.

5. Conclusions

Purine nucleotide and nucleotide-related analytes dramatically enhance the TICT-type fluorescence of dye **1**, whereas pyrimidine nucleotides have virtually no effect on the fluorescence of **1** suggesting a specificity of **1** for purine over pyrimidine analytes. However, relatively high concentrations of purine analytes are required to induce these changes, because of the modest association constants for **1** with these analytes. Although the fluorescence enhancements induced by cAMP and cGMP are greater than those induced by other purine analytes, the ability of **1** to distinguish between different purine analytes is somewhat limited. Nonetheless, in combination with other molecular structures designed to provide more specific recognition, this fluorescent dye might form the basis of a fluorescent chemosensor for purine nucleotides.

Fluorescent dye **1** possesses several features that make it attractive for potential use in laboratory practice, especially for biological applications. Dye **1** exhibits an intense absorption band in the visible region (Fig. 2) which should have significant excitation using standard argon, argon/krypton, or conventional lamp sources. The long wavelength fluorescence of **1** (608–613 nm, Fig. 3(a)), generated by exciting at 469 nm, reduces interference from cell or tissue autofluorescence (occurring around 460 nm), and provides a large Stokes' shift, separating excitation from emission wavelengths. This emission, together with the dual fluorescence obtained by exciting at 360 nm, also provides an opportunity for internal calibration by the ratioing of signals at two excitation or two emission wavelengths, cancelling out irrelevancies such as cell thickness, dye concentration, excitation intensity variations and detection efficiency [1]. The fluorescence quantum yield responses to the nucleotide and nucleotide-related analytes show insignificant fluctuations in the physiological pH range of 6–8 (Table 2). In addition, experiments with a very similar family member, *trans*-4-(*p*-*N*,*N*-dimethylaminostyryl)-*N*-phenethylpyridinium bromide have shown that these dyes are generally capable of diffusing across the cell membrane, are non-toxic to cells, and do not interfere with the physiological functioning of cells. [8,31]

Acknowledgements

The authors thank the Respiratory Health Network of Centers of Excellence for financial support of this work, and the Canadian Cystic Fibrosis Foundation for studentship support for P. Turkewitsch. We would like to acknowledge the contributions of the late Dr. Seymour Heisler. We thank Dr. F. Sauriol for assistance with NMR measurements, and

Dr. J. Silvius for assistance with equations. We are grateful to Dr. P. Hurst and R. Ganju for stimulating and helpful discussions.

References

[1] A.W. Czarnik (Ed.), Fluorescent Chemosensors for Ion and Molecule Recognition ACS Symposium Series 538, American Chemical Society, Washington, DC, 1993.
[2] S. Fery-Forgues, M.-T. Le Bris, J.-P. Guette, B. Valeur, J. Phys. Chem. 92 (1988) 6233–6237.
[3] M.D. Shin, D.G. Whitten, J. Phys. Chem. 92 (1988) 2945–2956.
[4] M.S.A. Abdel-Mottaleb, A.M.K. Sherief, A.A. Abdel-Azim, M.M. Habashy, L.F.M. Ismail, J. Photochem. Photobiol. 44 (1988) 161–169.
[5] K.Y. Law, Photochem. Photobiol. 33 (1981) 799–806.
[6] R.O. Loutfy, Pure Appl. Chem. 58 (1986) 1239–1248.
[7] C.V. Kumar, R.S. Turner, E.H. Asuncion, J. Photochem. Photobiol. A: Chem. 74 (1993) 231–238.
[8] E.C.S. Chan, B.R. Stranix, G.D. Darling, P.B. Noble, Can. J. Microbiol. 42 (1996) 875–879.
[9] V. Montana, D.L. Farkas, L.M. Loew, Biochemistry 28 (1989) 4536–4539.
[10] W. Rettig, Angew. Chem. Int. Ed. Engl. 25 (1986) 971–988.
[11] K. Bhattacharyya, M. Chowdhury, Chem. Rev. 93 (1993) 507–535.
[12] J.F. Létard, R. Lapouyade, W. Rettig, J. Am. Chem. Soc. 115 (1993) 2441–2447.
[13] B. Wandelt, P. Turkewitsch, B.R. Stranix, G.D. Darling, J. Chem. Soc., Faraday Trans. 91 (1995) 4199–4205.
[14] M.S.A. Abdel-Mottaleb, Laser Chem. 4 (1984) 305–310.
[15] M.S.A. Abdel-Mottaleb, A.M.K. Sherief, L.F.M. Ismail, F.C. De Schryver, M.A. Vanderauweraer, J. Chem. Soc., Faraday Trans. 85(2) (1989) 1779–1788.
[16] J.G. Darnell, H. Lodish, D. Baltimore, Molecular Cell Biology, 3rd ed., Scientific American Books, New York, 1994.
[17] P. Turkewitsch, B. Wandelt, G.D. Darling, W.S. Powell, Anal. Chem. 70 (1998) 2025–2030.
[18] P. Turkewitsch, B. Wandelt, R.R. Ganju, G.D. Darling, W.S. Powell, Chem. Phys. Lett. 260 (1996) 142–146.
[19] A.N. Kost, A.K. Sheinkman, A.N. Rozenberg, J. Gen. Chem. USSR (Eng. Transl.) 84 (1964) 4106–4112.
[20] C.A. Parker, W.T. Rees, Analyst 85 (1960) 587–600.
[21] C. Reichardt, Solvent Effects in Organic Chemistry, Verlag Chemie, New York, 1979, pp. 270–272.
[22] R. Lapouyade, K. Czeschka, W. Majenz, W. Rettig, E. Gilabert, C. Rullière, J. Phys. Chem. 96 (1992) 9643–9650.
[23] J.R. Lakowicz, Principles of Fluorescence Spectroscopy, Plenum Press, New York, 1983, pp. 187–215.
[24] R.S. Moog, N.A. Burozski, M.M. Desai, W.R. Good, C.D. Silvers, P.A. Thompson, J.D. Simon, J. Phys. Chem. 95 (1991) 8466–8473.
[25] M. Meyer, J.C. Mialocq, B. Perly, J. Phys. Chem. 94 (1990) 98–104.
[26] Y. Kato, M. Morgan Conn, J. Rebek Jr., , J. Am. Chem. Soc. 116 (1994) 3279–3284.
[27] M.W. Hosseini, A.J. Blacker, J.M. Lehn, J. Am. Chem. Soc. 112 (1990) 3896–3904.
[28] H. Kawai, T. Nagamuar, Mol. Cryst. Liq. Cryst. 267 (1995) 235–240.
[29] K.R.A. Samankumara Sandanayake, K. Nakashima, S. Shinkai, J. Chem. Soc., Chem. Commun. 1994 1621–1622.
[30] G.L. Duveneck, E.V. Sitzmann, K.B. Eisenthal, N.J. Turro, J. Phys. Chem. 93 (1989) 7166–7170.
[31] G.D. Darling, S. Heisler, B.R. Stranix, P. Turkewitsch, B. Wandelt, Viscosity Probe, Great Britain patent application #9 316 789.8, filed 1993/08/12, US patent application #289 062, filed 1994/08/11.